УДК 553.067
DOI 10.31242/2618-9712-2020-25-2-2

Immiscible silica- and iron-rich melts at the Kildyam volcano complex (central Yakutia, Russia)

A.V. Kostin

Diamond and Precious Metal Geology Institute SB RAS, Yakutsk, Russia
a.v.kostin2006@rambler.ru

Abstract. *A Kildyam Volcanic Complex was discovered in the natural outcrops and quarries of the Kangalassky terrace in the left bank of the Lena River 26 km north of Yakutsk. The manifestations of volcanism are represented by magnetite rich lava flows, agglomerate, pyroclastic breccia and tuff of andesites and dacites. Kildyam iron oxide deposit has been interpreted as lava flows and feeder dykes formed from iron-rich pyroxenite magma as a result of liquid immiscibility. Associated with andesitic lavas mineralization occur as massive, tabular bodies and stratified pyroclastic ores. Our research confirmed that tholeiitic trend of iron-rich pyroxenites evolves towards two immiscible liquids – magnetite lava and melilitite matrix. Further evolution leads to the separation of native iron and the transition of lavas to the calc-alkaline trend. Immiscibility of iron- and silica-rich melts during andesitic volcanism led to the formation of exotic varieties of magnetite-rich volcanic rocks. Fe-Ti-spinel mineral group is widespread at the Kildyam Volcanic Complex in the host andesite and in the local magnetite orebodies. The presence of native iron liquids as melt inclusions in clinopyroxene and plagioclase phenocrysts, magnetite- and silica-rich globules in andesite matrix, demonstrates the occurrence of liquid immiscibility in the early stage evolution of tholeiitic magmas. Lava flows saturated with native iron, magnetite, troilite and pyrite, native iron usually spherical in shape. According to microprobe analysis native iron contains Co – 0.04–2.89 %; Ni – 0.01–1.09 %; Pt – up to 1.45 %; Ir – up to 2.97 %; Pyrite contains Au – 0.11–2.25 %; Pt – 0.57–2.88 %; Ag – 0-1.18 %; Troilite contains Au – 0–3.15 %; Pt – 0–2.02 %; Ag – 0–1.68 %. In some parts of lava flows the amount of the magnetic fraction reaches 25–37 % of the total volume. In andesitic variolithic lavas the Pt content determined by the ICP-MS method – 0.11 g/t. A mineral phase enriched in Au (6.85 %) and Hg (2.94 %) was diagnosed in the* Fe_2TiO_4 – $MgAl_2O_4$ *spinelide. On the flanks of the volcanic field, alluvial gold is known in the Zolotinka stream (Cape Kangalassky) and in Paleogene sediments, discovered by the Khatyng-Yuryakh quarry 8 km from the center of Yakutsk by A.P. Smelov and A.A. Surnin. Most of the analyzed gold fineness varies from 846 to 996. Among high-fineness gold there is an Ag alloy – electrum which is typical for gold-silver mineralization. Discovered andesite associated iron-oxide ± gold and silver mineralization in Central Yakutia allows to refer it to analogous El Laco deposit in High Andes.*

Key words: Kildyam Volcanic Complex, magnetite lava, iron, gold, Central Yakutia.

Acknowledgements. *This research was funded by Diamond and Precious Metal Geology Institute, Siberian Branch of the Russian Academy of Sciences, project number 0381-2019-004. The author express his gratitude to Dr. Valentin P. Afanasiev for his constructive comments and excellent suggestions that helped to improve the manuscript. I am grateful for the support of the idea of studying the Kildyam Volcanic Complex and numerous discussions on all aspects of volcanism to the Institute colleagues – Vera A. Trunilina, Oleg B. Oleinikov and Vitaliy S. Grinenko. Larisa T. Galenchikova is thanked for excellent chemical analyses of rocks, Anna S. Vasileva – for gold and iron analyses, Nadejda V. Zajakina and Tatyana I.Vasileva – for x-ray analyses of volcanic rocks. Microprobe analyses were provided with the great help of Maria S. Jelonkina. Sample preparation for microscope and microprobe studies were well done by Vladimir Kurchatov.*

Introduction

Volcanic processes occurring in platform areas are of significant interest in modern geology due to their link with many deposit styles [1]. Volcanic manifestations were noted earlier in the Vilyui syncline and its frame [2]. For all the years of research, a significant number of the outcrops with volcanic tuffs were discovered, and not a single volcanic

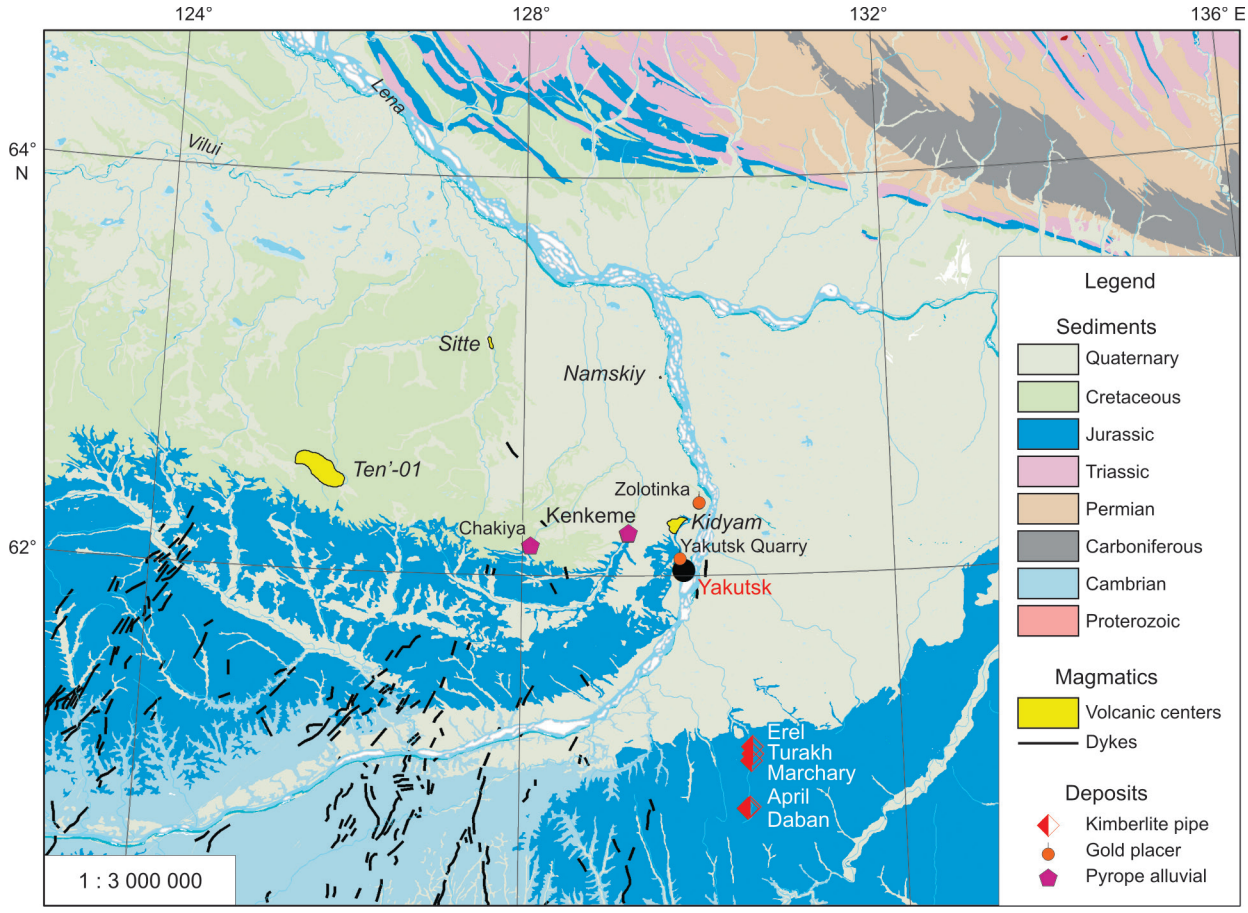

Fig. 1. Geological map of the Lena-Vilyui watershed, showing the location of Ten'-01 and Kildyam volcanic areas (geology simplified from mapping after Grinenko et al. [16]) and close up position to the mafic dyke swarms of the Vilyui rift [20]. Location of alluvial pyrope from lherzolite paragenesis after Afanasiev et al. [21]. Placer gold location from Smelov and Surnin [22]; Kimberlite pipes location from DPMGI SB RAS open-file report http://diamond.ysn.ru/wp-content/pdf/nir/Otchet-0381-2014-0004-2016.pdf.

structure was found. To date, the main volcanic centers of the Lena-Vilyui watershed are presented on Figure 1, were Ten'-01 and Kildyam are the discovered volcanic structures [3, 4].

The Sitte manifestation [N63.18°; E127.61°] was first described by Goldbraikh [5] as a 10 m outcrop of tufogenic rocks in Sitte river watershed. The sharply angular, bizarre shape of the pyroclastic material indicates the proximity of the volcanic source. Tuffs contains fern fossils flora of *Coniopteridium* and *Adiantites*, assigned to the Khatyryk Formation of Lower Cretaceous.

In the Namsky well [N63.00°; E129.50°], drilled to a depth of 2136 m [6] described a 4-meter layer of andesitic tuffs at the base of the Khatyryk Formation of Lower Cretaceous.

Volcanic cone Ten'-01 [N62.50°; E125.73°] and the Tyugeninsky Volcanic Complex [N62.56°; E125.76°], discovered by A.V. Kostin et al., in the sources of the p. Tyugene, forms a large volcanic center elongated in the north – west direction [7]. Andesites lies on the sediments of the Batylykh Formation (145.8–124.5 ma), reduced in Agrafen time (104–93.5 ma) and Chirima time (93.5–86.6 Ma). The dacite volcanic cone breaks through all these sediments.

Volcanic rocks of the Kildyam Volcanic Complex [N62.25°; E129.70°], were first described by A.V. Kostin and V.A. Trunilina [4]. The sediments are represented by sandstones and sand with interlayers and strata of siltstones, mudstones and coals of the Lower Vilyui, Marykchan and Bergein undivided formations of the Upper Jurassic. In the Upper Jurassic stratigraphic section, previously unknown stratified andesite-dacite lava flows with a visible thickness of more than 10 m were discovered. Due to numerous quarries in the Bolshoy Yakutsk area, it became possible to study the volcanic rocks of the Kildyam Volcanic Complex and discover that many fragments of lava are highly mag-

netic. Chemical analysis of magnetic varieties of lavas showed the presence of FeO_{total} from 21.46 to 70.8 %. Microprobe analysis confirmed presence of Cu-Co-Ni-bearing magnetite as a main mineral in lavas. Magnetite is associated with ulvospinel and contains impurities of Ag-tetrahedrite, acanthite, galena, sphalerite and chalcopyrite. Immiscibility of silicate liquids in Kildyam andesite lavas are manifested with globules of silica, plagioclase, magnetite and native iron. In different lava flows, globules are surrounded by K-plagioclase and melilite. Phenocrysts in magnetite lava are represented by the pyroxene, with native iron and troilite globules.

Many of the magnetite rich Kildyam lava features are typical for a Kiruna style deposits, which are widely recognized as a part of IOCG clan with prevailing of magnetite mineralization and occurs in a number of locations in the world. They range from Proterozoic to Holocene, and are associated with volcanic rocks or sub-volcanic intrusions [8–10]. Large accumulations of magnetite have been interpreted as having formed by crystal fractionation or by melt immiscibility between a silicate and an iron oxide melts. Philpotts [11, 12], Tornos et al., [13] propose that melt inclusions in plagioclase and pyroxene phenocrysts are tipical for Kiruna-type deposits and confirms the role of silicate liquid immiscibility in the formation of iron-rich ore. According to this view, iron-oxide ore formed at the same time and by the same processes as the host volcanic rocks.

This paper is devoted to the Kildyam Volcanic Complex in Central Yakutia with high grade iron-oxide ore mineralization within lava flows that have share many common features with a Kiruna-type iron oxide deposit, characterized by a high content of magnetite.

Geological setting

The geology of the Lena-Vilyui watershed has been described in detail by L. M. Parfenov, A.V. Prokopiev, V.V. Gaiduk [14], L.M. Parfenov [15], V.M. Grinenko et al [16–18]. The Leno-Vilyui basin, consisting of the Vilyui syneclise and the Pre-Verkhoyansk deflection, is made of the Upper Jurassic – Lower Cretaceous boundary rocks (Laptev and Kitchan subcomplexes of the Verkhoyansk terrigenous complex) within the eastern Siberian platform. Its folded framing was studied both from natural outcrops in the river basins of Vilyui, Lena and Aldan and from deep horizons using samples obtained by core drilling [16]. Based on materials from past geological surveys [16], rocks of the left bank of the river Lena at Kildyam site [N62.25°; E129.70°] are represented by sandstones and sands with interbeds and stratas of siltstones, mudstones and coals of the Lower Vilyui, Marykchan and Bergein undivided suites of the Upper Jurassic (J_3nv-br). The Marykchan Formation is composed of dark gray and black mudstones and siltstones, often carbonaceous, with thin layers of fine-grained light gray sandstones. The suite includes several lenses and interlayers of brown coal. According to the Bergein Formation, it consists of thick strata of light gray, almost white sandstones interbedded with dark gray siltstones and black carbonaceous mudstones. The suite contains several coal seams.

Until recently, the southeastern flank of the Vilui Basin did not attract attention of geoscientists in terms of any volcanic activity. Volcanic activity of the southeastern flank of the Vilui Basin has been first recognized in 2014, after discovering volcanic structure Ten'-01 (volcanic cone coordinates are N62.50°; E125.72°), with dacite lavas and crystalloclastic tuffs in the Upper Jurassic section of primary sedimentary terrigenous continental rocks at the boundary with the Lower Cretaceous continental terrigenous sediments [3].

In 2016–2019, the Diamond and Precious Metal Geology Institute (Yakutsk, Russia) conducted geological survey at the left bank of the Lena River at the slope of the Kangalassky terrace 26 km north of Yakutsk (the Bolshoy Yakutsk area). A numerous previously unknown outcrops with wide spread of andesitic and dacitic lavas and subvolcanic rocks at Kildyam site were discovered [4]. Geological map (Fig. 1) showing the location of main volcanic centers and spatially associated alluvial placer pyrope and gold manifestations. Recently discovered kimberlite pipes Erel, Turakh, Manchary, April and Daban [19] are located southeast from Yakutsk.

Methods and analytical techniques

Ninety-six representative surface samples of igneous rocks including different rock textures styles were collected during field works of 2016–2020. Samples of unaltered andesite from the Kildyam site were prepared for standard petrographic study and examined in polished thin sections, using reflected and transmitted light microscopy. The following methods were used during the study of the Kildyam Volcanic Complex.

First, detailed field mapping was performed using ArcGis images to identify rock location in regional structures. Volcanic flows morphologies were

Representative chemical analyzes of major oxides (wt. %) and results

Sample	1033/3	1037/2	1042/2	1033/5	1044/4	1044/5
	1	2	3	4	5	6
SiO_2	70.29	73.27	71.31	66.34	63.9	64.88
TiO_2	0.9	0.12	0.15	1.03	0.92	0.7
Al_2O_3	15.72	15.35	15.74	17.81	19.05	16.58
Fe_2O_3	1.97	0.12	1.74	4.54	0.71	4.14
FeO	0.57	1.53	0.83	0.42	5.51	3.73
MnO	0.06	0.08	0.02	0.1	0.13	0.15
MgO	0.78	0.75	0.95	1.41	1.84	1.34
CaO	2.07	1.17	1.34	1.86	1.36	1.47
Na_2O	3.06	3.19	3.36	2.52	2.3	2.94
K_2O	2.88	3.56	3.72	2.94	3.61	3.44
P_2O_5	0.35	0.12	0.13	0.42	0.22	0.24
$H2O^+$	1.1	0.47	0.04	0	0.23	0
$H2O^-$	0.78	0.04	0.12	0.42	0	0.1
CO_2	0.44	0.23	0.26	0.22	0.38	0.23
S	0.12	0.01	0.02	0.03	0.1	0.06
LOI	0	0	0.27	0.42	0	0
Total	**99.53**	**99.93**	**99.76**	**99.64**	**100.26**	**99.80**
La	70.71	56.69	50.18	48.47	66.37	59.20
Ce	137.44	102.24	95.81	99.32	119.71	106.07
Pr	15.02	11.01	10.56	11.23	13.97	12.44
Nd	54.72	41.52	35.86	40.22	53.06	50.35
Sm	8.47	5.35	5.67	5.64	7.96	6.97
Eu	1.59	1.25	1.28	1.42	1.78	1.41
Gd	7.56	4.87	5.25	5.82	7.05	6.65
Tb	0.85	0.61	0.66	0.68	1.05	0.79
Dy	4.92	3.28	2.87	3.62	5.37	4.13
Ho	0.80	0.52	0.54	0.65	1.05	0.78
Er	2.12	1.47	1.48	1.54	2.82	1.99
Tm	0.29	0.18	0.21	0.20	0.41	0.27
Yb	1.97	1.22	1.14	1.30	2.37	1.67
Lu	0.33	0.18	0.23	0.20	0.43	0.28
Cs	1.19	0.97	1.11	1.77	3.93	2.31
Hf	3.11	1.93	1.75	2.26	3.47	2.68
Ta	1.93	1.18	1.40	1.19	1.46	1.28
Th	16.22	12.44	10.98	10.62	25.29	14.56
U	2.56	1.70	1.82	2.34	4.77	2.92
Ba	1206.54	1372.39	1233.14	1249.43	1232.95	1314.02
Rb	89.28	93.86	89.17	104.08	122.14	99.36
Sr	376.85	375.81	378.46	348.31	262.99	308.17
Y	22.66	13.61	13.82	14.97	25.91	18.59
Zr	70.40	46.02	32.49	42.20	90.33	61.71
Nb	20.35	12.43	14.71	13.20	16.86	14.92
Pt	–	–	–	–	–	–

Samples: 1033/3 – Yellow tuff sandstone. 1037/2 – Coarse-grained gray volcanic tuff. 1042/2 – Red volcanic tuff. Dacite series: 1033/5 – Banded dark gray lava-breccia. 1044/4 – Volcanic tuff with the remains of flora. 1044/5 – Black pumice. 1031/1 – Banded lava-breccia. 1031/2 – Partially altered black and red lamellar breccia. 1044/2A – Porous lava. Andesite series: 1030/4A and

Table 1

for trace elements (g/t) for the rocks of Kildyam Volcanic Complex

1031/1	1031/2	1044/2A	1030/4A	1030/8	1039	1042/3
7	8	9	10	11	12	13
69.02	63.38	67.25	56.02	56.38	40.17	0.65
0.16	0.14	0.84	0.69	0.16	0.19	0.07
16.18	15.72	17	13.45	12.98	8.58	0.62
0.31	9.68	1.23	1.57	0.65	14.19	93.66
3.38	0.86	2.71	7.2	4.93	18.23	0.42
0.07	0.3	0.13	0.35	0.3	1.6	3.06
1.15	1.1	1.6	2.03	2.62	1.69	0.9
1.43	1.25	1.53	12.12	16.32	13.01	0.51
3.2	2.77	3.06	1.9	2.16	0.26	0.09
3.44	3.24	3.41	2.05	2.05	0.18	0.03
0.28	0.21	0.28	0.14	0.07	0.01	0.09
0.62	0.74	0.66	0.39	0.46	0.84	0.05
0.18	0.12	0.12	0.48	0.14	0.5	0.06
0.09	0.13	0.31	0.27	0.2	0.78	0
0	0.04	0.04	0.35	0.3	0.35	0.03
0.35	0.1	0	0.8	0.07	0	0
99.5	**99.54**	**99.93**	**98.85**	**99.51**	**100.08**	**100.18**
49.52	62.59	62.73	69.35	69.23	34.53	9.73
100.76	119.93	129.39	131.07	136.00	58.71	19.19
11.48	13.47	14.75	15.61	16.90	6.55	2.53
42.25	49.49	50.64	66.98	71.05	23.12	10.88
6.17	7.59	7.51	11.90	11.12	4.12	2.08
1.48	1.42	1.73	2.57	2.99	0.80	0.69
5.59	6.69	7.07	13.75	13.93	4.69	3.27
0.72	0.89	0.90	1.99	2.00	0.68	0.69
3.89	4.35	4.68	12.85	13.34	4.66	5.22
0.61	0.76	0.73	3.04	2.90	0.98	1.28
1.66	2.12	2.01	8.78	8.44	2.43	4.73
0.24	0.31	0.30	1.26	1.26	0.40	0.77
1.54	1.41	1.74	9.20	8.93	2.44	5.80
0.21	0.23	0.25	1.53	1.45	0.47	0.90
1.77	2.04	2.12	1.14	1.32	0.32	0.03
1.99	1.66	2.64	9.92	9.46	10.38	1.22
1.35	1.12	1.61	1.28	1.31	1.33	0.17
10.70	12.63	16.49	16.42	15.79	17.36	3.79
2.56	2.67	3.29	5.99	6.14	4.60	0.80
1274.78	1242.82	1129.17	4562.00	4199.34	3026.24	77.00
100.25	94.74	98.76	48.96	54.65	7.91	2.16
390.16	327.87	310.46	2693.85	2653.61	2078.70	30.72
17.02	19.85	18.92	103.79	103.21	27.78	34.39
45.94	42.88	55.82	313.57	295.24	313.92	85.59
15.85	12.74	18.44	16.14	15.84	14.50	1.87
–	–	–	0.11	0.11	–	–

1030/8 – Variolitic bubbly gray lava with native iron. Ultramafic series: 1039 – Subvolcanic pyroxenite. Magnetite series: 1042/3 – Magnetite ore in lava.

described, and the lateral or vertical successions of lithofacies were used to identify volcanic units. Then sample collection of the leaf flora fossils in the red and reddish-brown crystalloclastic volcanic tuffs and an age determination by V.S. Grinenko in DPMGI SB RAS and A. Kirichkova in St. Petersburg, VNIGRI [23].

Second, a field collection of rock samples was created to characterize lithotype, textural, and structural features. All chemical analyses of volcanic rocks were carried out at the Diamond and Precious Metal Geology Institute, Siberian Branch, Russian Academy of Sciences (DPMGI SB RAS). The major oxides compositions were analyzed using methods of spectrometry, atomic emission spectrometry, ionometry with ion-selective electrode, gravimetry and titrimetry. The major analyzed oxides were: SiO_2, TiO_2, Al_2O_3, Fe_2O_3, FeO, MnO, MgO, CaO, Na_2O, K_2O and P_2O_5. The loss on ignition (LOI) values ranges from 0 to 0.8 %. Trace elements were analyzed by inductively coupled plasma mass spectrometry (ICP MS) in the chemical analytical center «Plasma», Tomsk, Russia. Analyzed trace elements were: La, Ce, Pr, Nd, Sm, Eu, Gd, Tb, Dy, Ho, Er, Tm, Yb, Lu, Cs, Hf, Ta, Th, U, Ba, Rb, Sr, Y, Zr, Nb and Pt.

Third, microscopic petrography and microprobe analysis of 77 polished sections was conducted to provide detailed data to confirm the phenocrysts and glass chemistry, presence of magnetite and other ore minerals. All microprobe and x-ray analyses were carried in the Diamond and Precious Metal Geology Institute, Siberian Branch, Russian Academy of Sciences (DPMGI SB RAS). Samples were prepared from polished sections with a sprayed thin conductive layer of carbon. Back-scattered electron (BSE) images and spot analyses of minerals were done using scanning electron microscope JSM-6480LV with energy spectrometer INCA-Energy, accelerating voltage at the cathode 20 kV. Major minerals in lavas were determined by x-ray phase analysis using D2 PHASER diffractometer.

Fourth, sampling of a magnetic fraction from a lava sample weighing 30 kg showed that at least 30 % of the sample weight is magnetic. For magnetic and non-magnetic varieties of lavas, a chemical analysis was performed. Polished samples were prepared from magnetic varieties of rocks for microscope and microprobe studies. For magnetite lavas, the chemical composition of the matrix was obtained by areal microprobe scanning.

Volcanic formations

A Kildyam is a Late Jurassic–Early Cretaceous volcanic complex in the transition zone between the Siberian platform and the Verkhoyansk-Kolyma folded region in Central Yakutia [3, 23]. It consists of several small eruptive centers with a conical morphology and fissure outpourings of lavas. The outcrops showing that dacite lavas first penetrate through Late Jurassic sandstones (3.0 m) along a fissure conduit and then cover the sandstones with 2–5 m layer. Lava flow is covered with a layer of crystalloclastic tuffs, about 1.5 m thick, which is brecciated by the next lava flow (Fig. 2). The Kildyam volcanic field covers 53.65 km^2 and has a lava volume at least 0.53 km^3. The chemical compositions of the main varieties of volcanic rocks are shown in the Table 1. They include volcanic tuff, pumice, lava, lava-breccia, ignimbrites of dacite series, lava and lava-breccia of andesite series, subvolcanic pyroxenite and magnetite lava.

Volcanic tuffs. The recognition that some of the inter-lava red beds are tuffs rather than laterites may imply complex volcanic lava successions within the Lena-Vilyui watershed. Volcanic tuffs are characterized by rough layering, their color varies from pale red to brick. They contrast with the dark-coloured lava and stand out well in ArcGis, Google and other space images among rocks of other colors (Figure 3, *A* and *B*). The same color of volcanic tuff characterizes many volcanic regions of Kamchatka, Armenia, Lassen National Park in Northern California, etc. It is assumed that the color of red tuffs is the result of temperature and fluid exposure to volcanic ash during volcanic eruptions [24] and later weathering [25]. Selective weathering changes iron oxidation state in volcanic tuffs from Fe^{+2} to Fe^{+3} form and tuffs color changes from dark-grey to reddish (Fig. 3, *C*).

Tuffs of the Kildyam Volcanic Complex have a lithocrystalline structure with ash cement. From 0.2 to 1 mm sized phenocrysts and angular fragments of crystals of plagioclase, weakly pelitized potassium feldspar and quartz, irregularly separated porphyry andesite and glass fragments are cemented by fine pyroclastic material saturated with iron hydroxides. The red and reddish-brown crystalloclastic volcanic tuffs of the Upper Jurassic flora contain fossils of leaf flora (Fig. 4) typical of the Bergeya Formation in the Aldan River basin. The age of the leaf flora was determined as Late Jurassic by A. Kirichkova in St. Petersburg, VNIGRI [23].

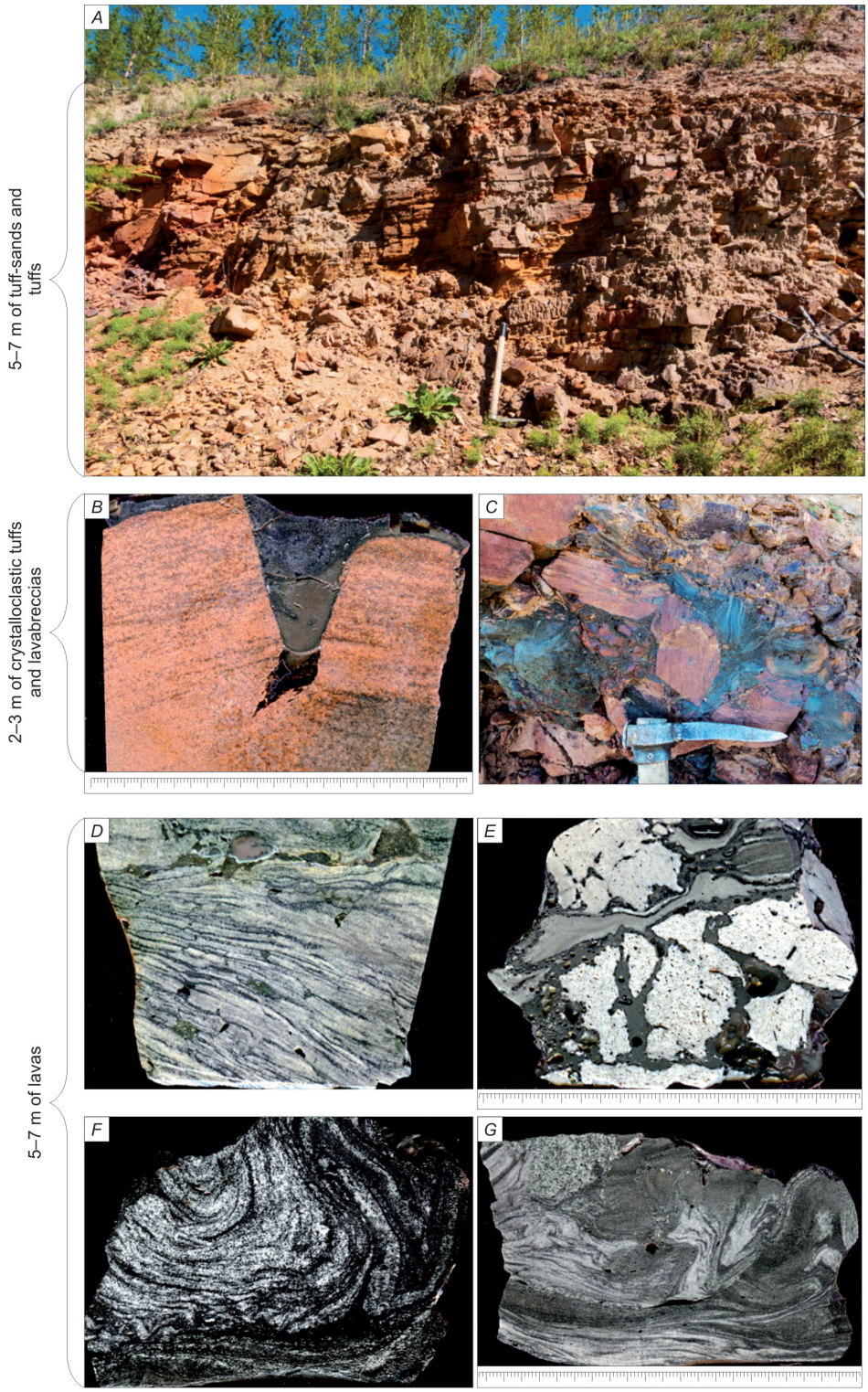

Fig. 2. Field photographs from the outcrop of volcanic formations in Kildyam Volcanic Complex (left side of the Lena River) and rock samples.
A – Outcrop of tuff-sands (yellow) and tuffs (reddish). *B* – Crack in crystalloclastic tuffs filled with lava. *C* – Lava flow brecciating a layer of crystalloclastic tuffs with leaf flora. *D* – Ignimbrites (sample 1044/3) were light – fragments of porous lava with crystallites, black – glass fragments and lenses elongated and flattened parallel to the surface of light porous lavas, brown – fayalite (Fa) segregations saturated with melted interspersed spinel and hematite. *E* – Brecciated lava with crystallites, dark – obsidian cement. *F* – Wavy lava (sample 1033/5) were light – lava with crystallites, dark – obsidian. *G* – Autobrecciation in the lava flow.

Fig. 3. One of the quarries on the Lena-Vilyui watershed where red tuffs are mined for road works.
A – ArcGis satellite image of a quarry and *B* – *A* photo of the open pit showing that red tuff color is a reliable prospecting tag. *C* – Selective weathering of volcanic tuff at Kildyam lava successions. *D* – The later lava flow (dark grey) brecciate red tuffs.

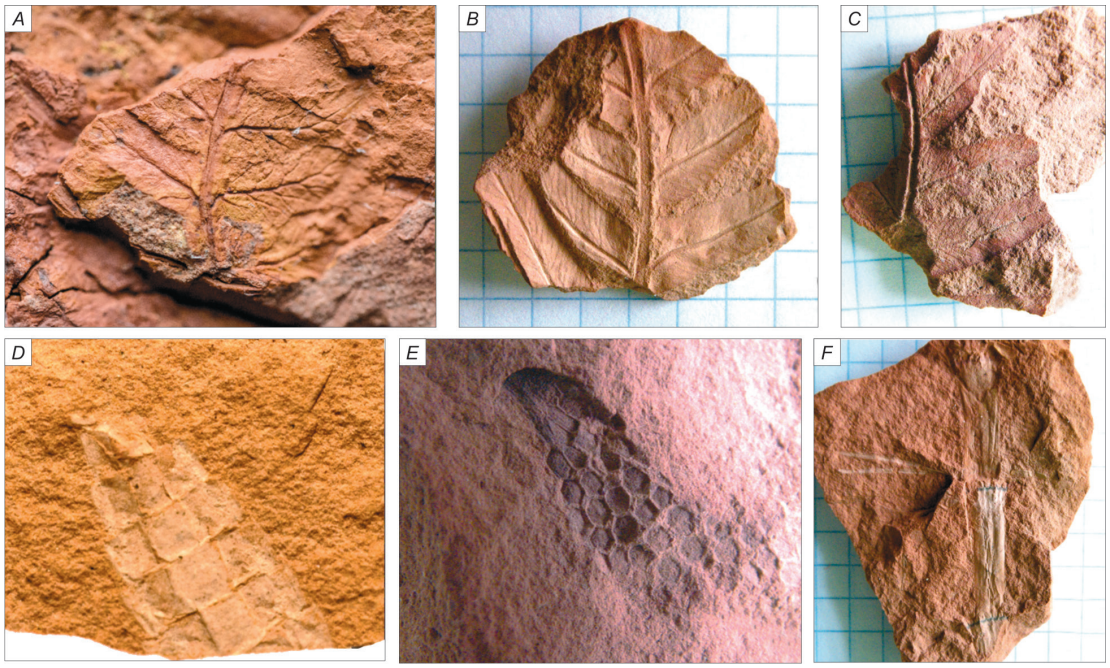

Fig. 4. The fossils of Late Jurassic flora in brick-red crystalloclastic tuffs from Kildyam volcanic field [23].
A–C – *Cladophlebis aldanensis* Vachr; *D* – *Cycadales megastrobil* imprint; *E* – *Coniferales megastrobil* imprint; *F* – *Equisetites* cf. *acmophyllus* Kiritch.

Lava breccias. Breccia facies are common at Kildyam Volcanic Complex and usually observed between sections of differing lava flow orientations. An 1–4 m wide breccia zone consist of angular fragments of hyalopilitic andesites or variolitic andesibasalts and reddish-brown crystallo-

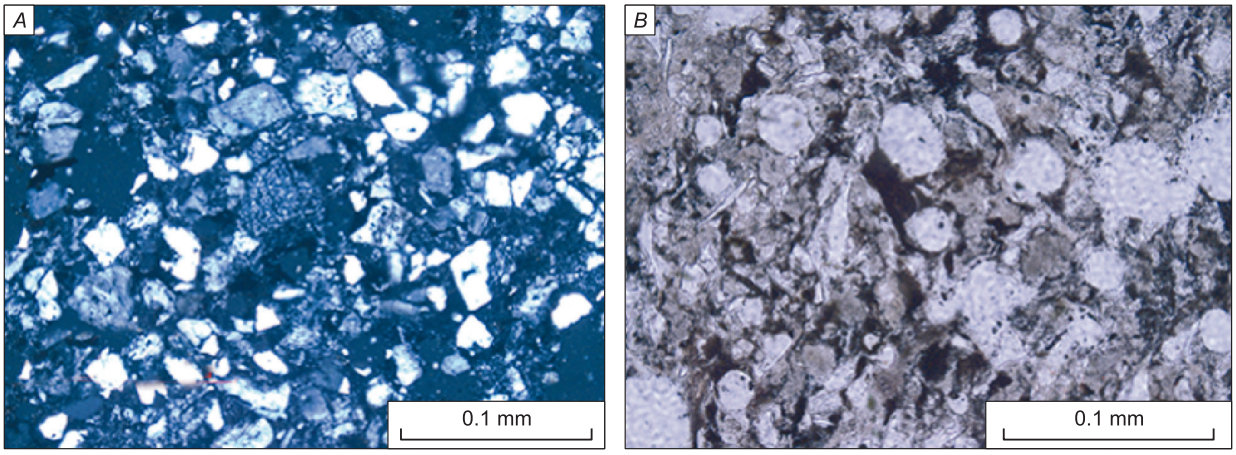

Fig. 5. Photomicrographs of dacite lava facies.
A – Dacite of vent facies, sample 1042/1. *B* – Dacite of lava facies, sample 1044/3.

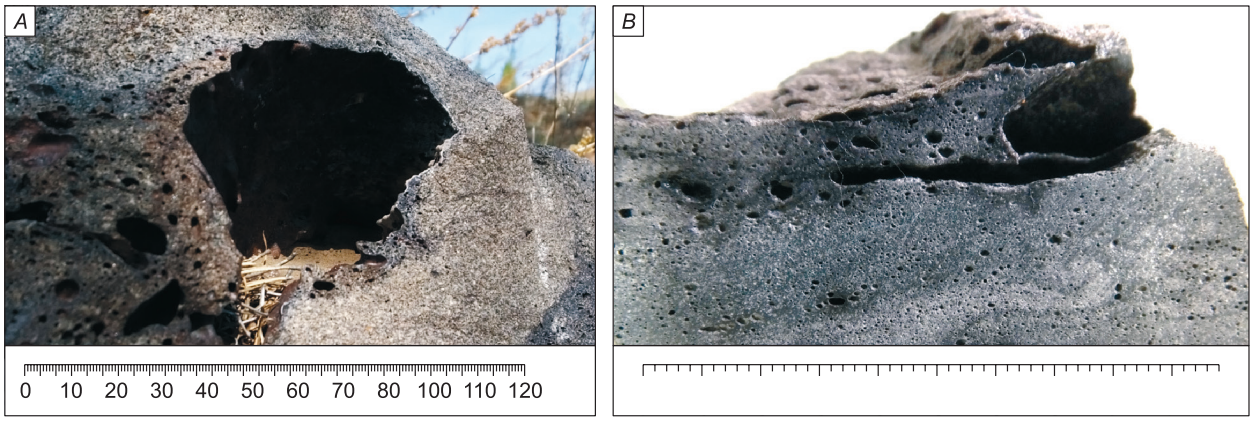

Fig. 6. Photographs of vesicles in the dacite lava flows. Spherical vesicle (*A*) and elongated vesicle (*B*) with no filling showing that gas release from melt caused the formation of primary porosity, while secondary hydrothermal alteration is absent.

clastic volcanic tuffs in bubble dacite-rhyodacite glass containing tiny feldspar microlites. The boundaries between the inclusions of rocks and glass are quite clear which is typical for sintered tuffs or ingimbrites (Fig. 2, *B*–*E*). A small amount of host sandstone in lava breccias is typical for Kildyam fractured lava outflows. The number of fragments of the host rock is higher in small dacite extrusions.

Dacites. Dacites are present in the extrusion of the Kildyam Volcanic Complex and in the outcrops in the walls of the quarries of the Namtsyrsky road. The first is dominated by dacites of the volcano vent facies, where the glassy felsitic bulk rock is overflowed with crystals and crystal fragments (prevail) of polysynthetically twined oligoclase-andesine, pelitized sanidine and quartz (Fig. 5, *A*). Lava facies dacites are bubbly to foamy, with feldspar and quartz crystals in a glassy to microfelsitic matrix with feldspar and light-colored amphibole microcrystallites (Fig. 5, *B*).

The formation of banded and undulating lavas is typical for the lava flows on the slopes of the Kildyam volcano. Lavas are characterized by the alternation of 1–15 mm thick light and dark stripes. The crystalline phase predominates in light finely porous bands, and is represented by feldspar and quartz. Dark bands are represented by obsidian or by bubbly riodacite with size of the voids larger than in the light bands and with the predominance of the glassy matrix over the crystalline phase (Fig. 2, *F* and *G*).

Bubble textures and shape in the Kildyam lava flows suggest two styles of solidification. In the first case, when the lava fills depressions in the relief and solidifies without movement, the major bubbles have round shapes. In the second case, when the lava flow was moving along the slope, the shape of the bubbles is elongated (Fig. 6).

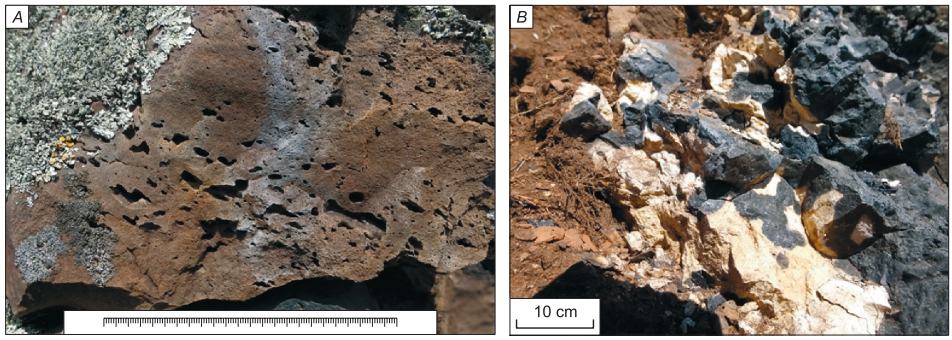

Fig. 7. The natural outcrops of the Kangalassky terrace with different styles of vesicles in Kildiam lavas:
A – Empty stretched vesicles in dacite. *B* – Complex shape of vesicles in dacite (black) filled with cristobalite (white).

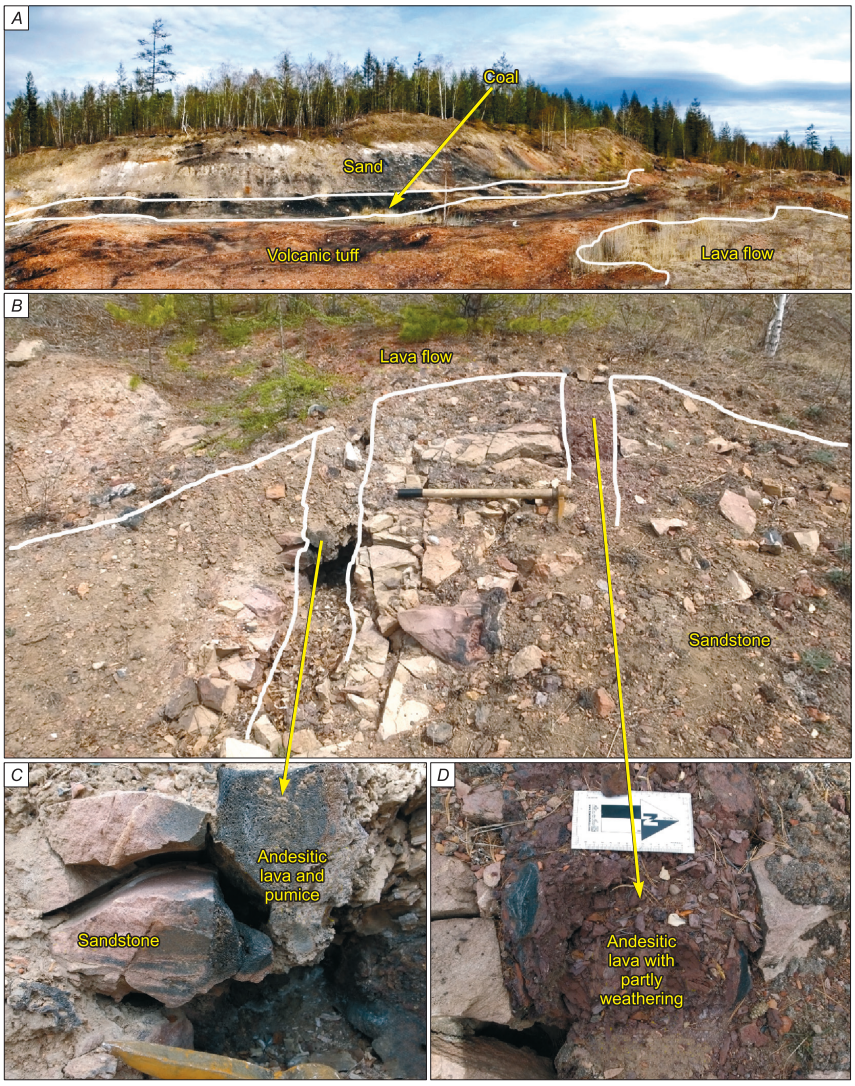

Fig. 8. One of the quarries with red tuffs at the Kangalassky terrace in the left bank of the Lena River (location N 62.18°; E 129.49°).
A – Sand, coal, red volcanic tuff with fossils of Late Jurassic flora and andesitic lava flow, mined from top to bottom in the quarry. *B* – Andesitic lava flow and related feeder dykes in steeply falling cracks discovered in the roof of a sandstone layer, covered with an andesitic lava flow. *C* – Feeder dyke-1 with porous andesite lava and pumice (black) in sandstone (light) crack. Close up to contact with the andesitic lava, sandstone is high temperature altered and changes color to pink. *D* – In the feeder dyke-2, close to the bottom of andesitic lava flow, lava is altered and weathered.

Detailed observations confirmed that vesicles in Kildiam dacites are empty or filled with a vapor-phase cristobalite (Fig. 7) that proves a local silica redistribution and magmatic degassing. The presence of cristobalite in volcanic rocks is considered an evidence of redistributed silica within the magmatic system [26–28]. We suggest that the presence of large clusters of cristobalite indicates a close proximity to the lava exit paths and empty bubbles indicate the distant lava flows.

Andesite. Volcanic structures, composed of andesite lavas, are represented by a series of small shafts with a flat outer and steep inner surface. Andesite lava eruptions of the Kildyam Volcanic Complex are confined to 0.2 to 1 m wide cracks (Fig. 8). Andesite is of variolitic texture lava with ovoidal segregations, submerged in a glassy or microcrystalline matrix, composed of intergrowths of needle-shaped clinopyroxene – diopside, wollastonite, less commonly hedenbergite, rarely augite and labrador crystals, with brown altered glass, Fe-rich olivine – fayalite is relatively less common. Andesitic lava has a density of 2.88–2.92 g/cm^3 and the Pt content of 0.11 g/t (determined by the ICP-MS method).

Petrographic and microprobe studies confirmed the liquid immiscibility in silicate melt during crystallization. Immiscible liquids are preserved as globules of one glass in another in andesites and as melt inclusions of native iron in matrix (Fig. 9).

Pyroxenite. Abundant pyroxenite xenoliths are discovered in a Kildyam dacite lava flow only from a single location at the N 62.29°; E 129.80°. The

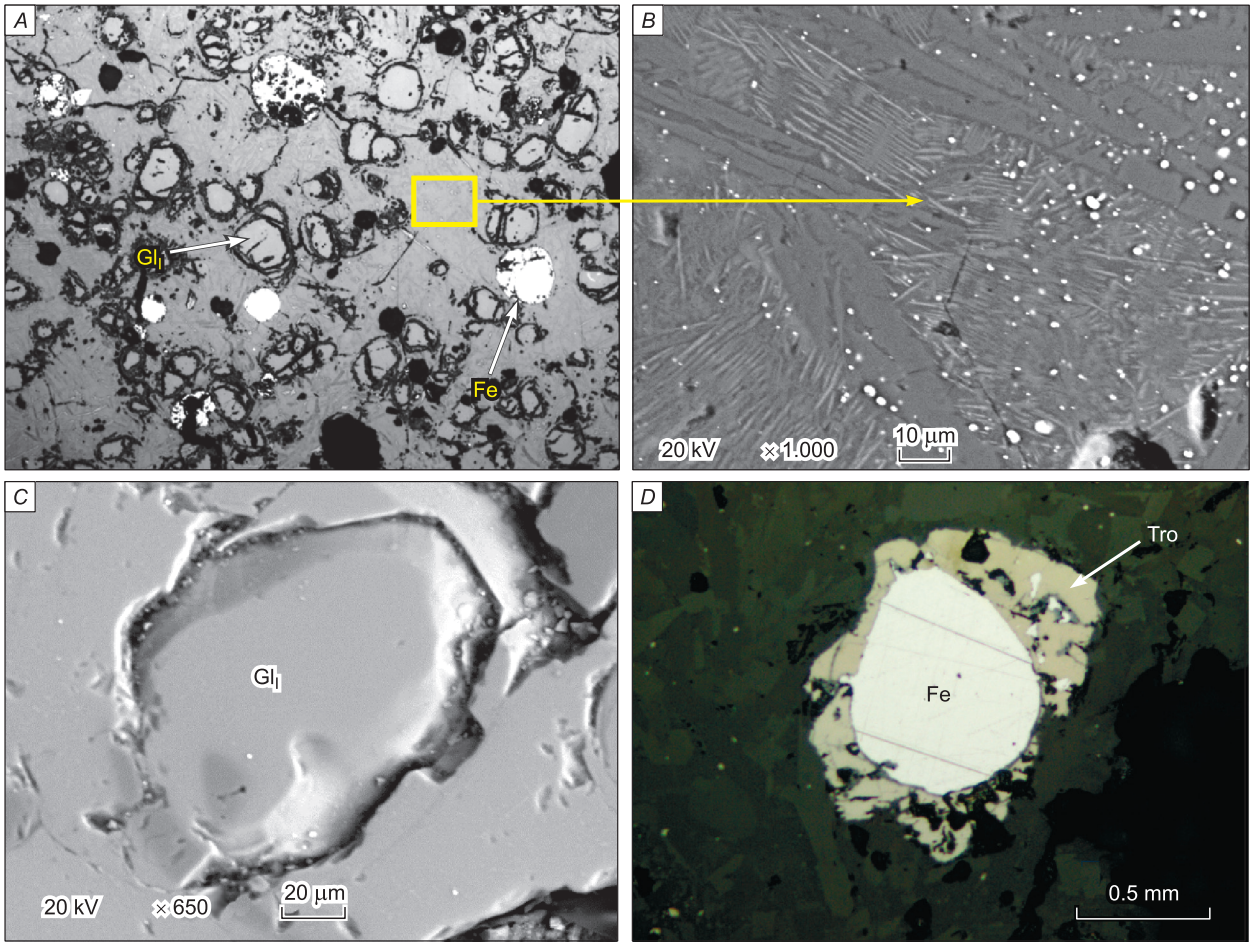

Fig. 9. A backscattered electron images (*A*–*C*) and photomicrograph (*D*) of variolitic andesite (sample 1030).
A – An overview shot showing the relationship of variolies, glass and native iron globules with microcrystalline matrix. Yellow rectangle shows the location of figure 9, *B*. *B* – Microcrystalline matrix with early-crystallized dendritic pyroxene forms and native iron melt inclusion in plagioclase-made glass is composed (in %) of: SiO_2 – 55.37, TiO_2 – 1.28, Al_2O_3 – 18.06, FeO_{total} – 13.21, CaO – 2.31, Na_2O – 4.74, K_2O – 4.7. *C* – Spherical globule [Gl_1] of glass is composed (in %) of SiO_2 – 56.54, TiO_2 – 0.78, Al_2O_3 – 14.37, FeO_{total} – 5.11, MgO – 2.28, CaO – 17.56, Na_2O – 2.24, K_2O – 1.33. *D* – Andesitic microcrystalline matrix with a drop of native iron in troilite surrounding. Abbreviations: Gl_1 – Globule-1; Fe – native iron, Tro – troilite.

edges of the pyroxenite fragments are slightly melted, and the crystalline structure of the rock is preserved inside completely. The melted reaction rim with the width of 1–5 mm on xenolite margin is dark colored as host dacites and can be recognized only in the polished sections. Pyroxenite is heavy (3.41 g/cm^3), fine-grained black rock of allotriomorphic and rarely panidiomorphic structure with FeO_{total} content > 32 % (sample 1039, Table 1).

Much attention needs to paid to a relationship between the pyroxenite xenoliths brought to the surface by volcanic eruption and lava style. Studies of pyroxenite xenoliths derived from lavas offer unique glimpses into the properties of the deep continental crust. The *P–T* conditions for magma generation level of the deep-seated xenoliths in lavas from the Lena-Vilyui watershed have been previously estimated as 12–8 kbar and 1200° C [29]. All found py-

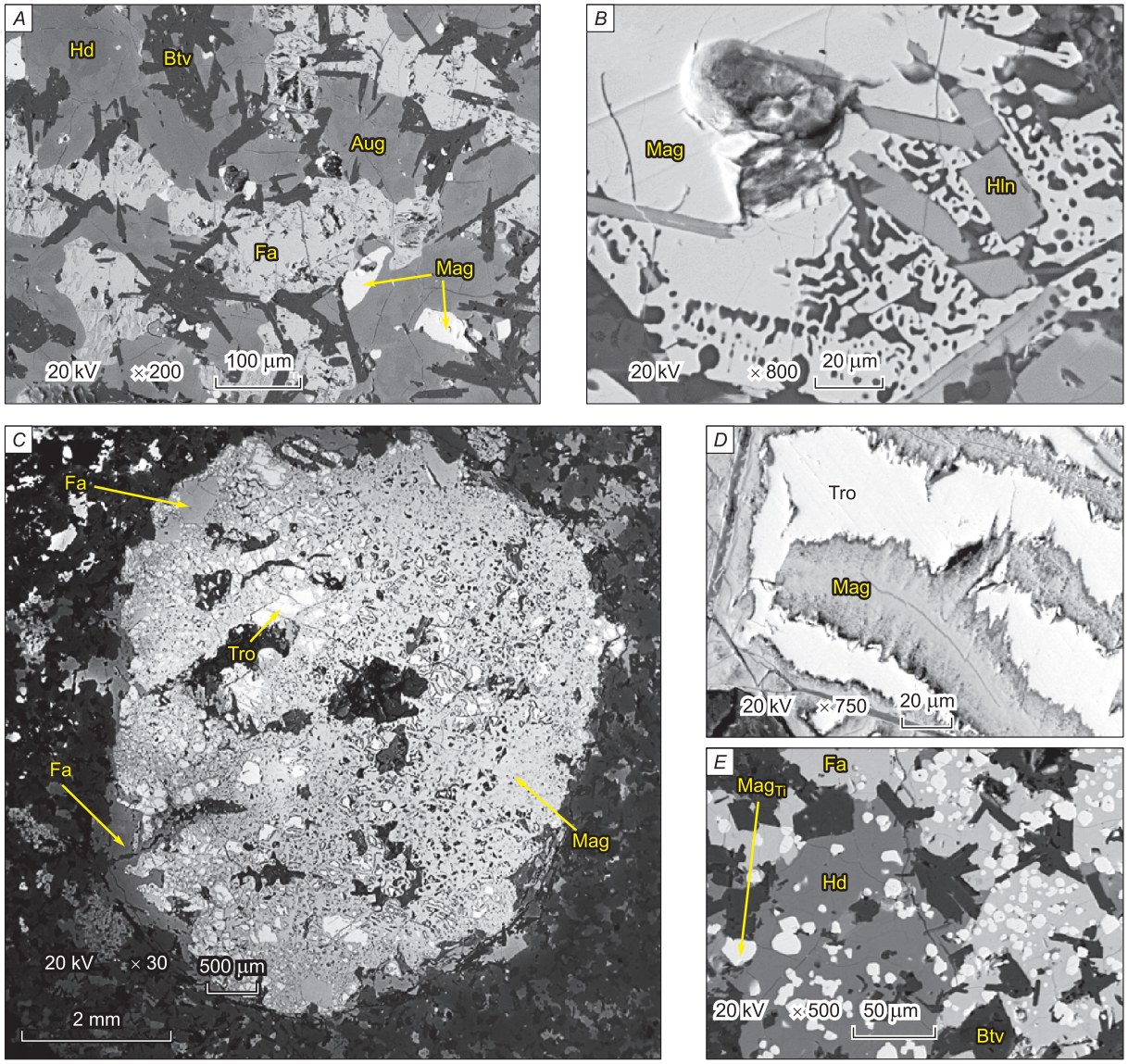

Fig. 10. A backscattered electron images showing ore minerals assemblages in pyroxenite matrix (sample 1039).
A – The relations between pyroxene, olivine, plagioclase and magnetite in pyroxenite xenolith. Magnetite is composed (in %) of: FeO_{total} – 85.38, TiO_2 – 11.16, Al_2O_3 – 2.54, MnO – 0.9. *B* – Intergrowth of magnetite crystal with rapid growth texture in the border and hyalophane. Hyalophane is composed (in %) of: SiO_2 – 51.71, Al_2O_3 – 21.94, FeO_{total} – 1.5, CaO – 1.9, BaO – 16.35, K_2O – 5.9. *C* – Ore globule in pyroxenite matrix is composed of fayalite, troilite and magnetite. *D* – Fragment of ore globule showing the intergrowth of troilite and magnetite. *E* – Fragment of ore globule-bearing matrix showing the high degree magnetite saturation of fayalite and hedenbergite. Abbreviations: Aug – augite, Fa – fayalite, Tro – troilite, Mag – magnetite, Hln – hyalophane, Hd – hedenbergite , Btv – bitownite.

roxenite samples are from 5 to 40 cm fragments in a dacite lava with cristobalite in vesicles (Fig. 7, *B*). There is reason to believe that this site is one of the local volcanic centers.

Based on mineral assemblage xenoliths can be referred to olivine clinopyroxenite. The rock composition includes 48.1 % of pyroxene (augite, rarely hedenbergite), 23.6 % of plagioclase (bitownite-anorthite), 16.8 % of olivine (average $Fo_{0.105}$ $Fa_{0.895}$), 6.07 % of magnetite, 1.79 % of calcite and 0.75 % of troilite. Less common minerals are Ba-feldspar celsian and K-Ba-feldspar hyalophane. Ore minerals are concentrated in up to 0.7 cm in size globules, surrounded by olivine rims. Ore globules are composed of magnetite and troilite in equal proportions.

Magnetite lavas. Immiscibility of iron- and silica-rich melts during andesitic volcanism led to the formation of exotic varieties of magnetite-rich volcanic rocks. Fe–Ti-spinel minerals group is widespread at the Kildyam Volcanic Complex in the host andesite and in the local magnetite orebodies. The iron-rich lava can be identified as two main types.

1. **Titaniferous magnetite iron ore.** There is abundant (up to 2 % by volume) iron mineralization disseminated in the andesite matrix. Fe-rich andesitic lava (type-1) includes native iron, troilite and mixture of ulvospinel (Fe_2TiO_4) with spinel ($MgAl_2O_4$). This spinel group includes Au-Hg mineral phase (Table 2, Fig. 9). Matrix is composed (in %) of: SiO_2 – 54.73, TiO_2 – 1.49, Al_2O_3 – 19.0, FeO_{total} – 12.79, CaO – 2.31, Na_2O – 5.17, K_2O – 4.52.

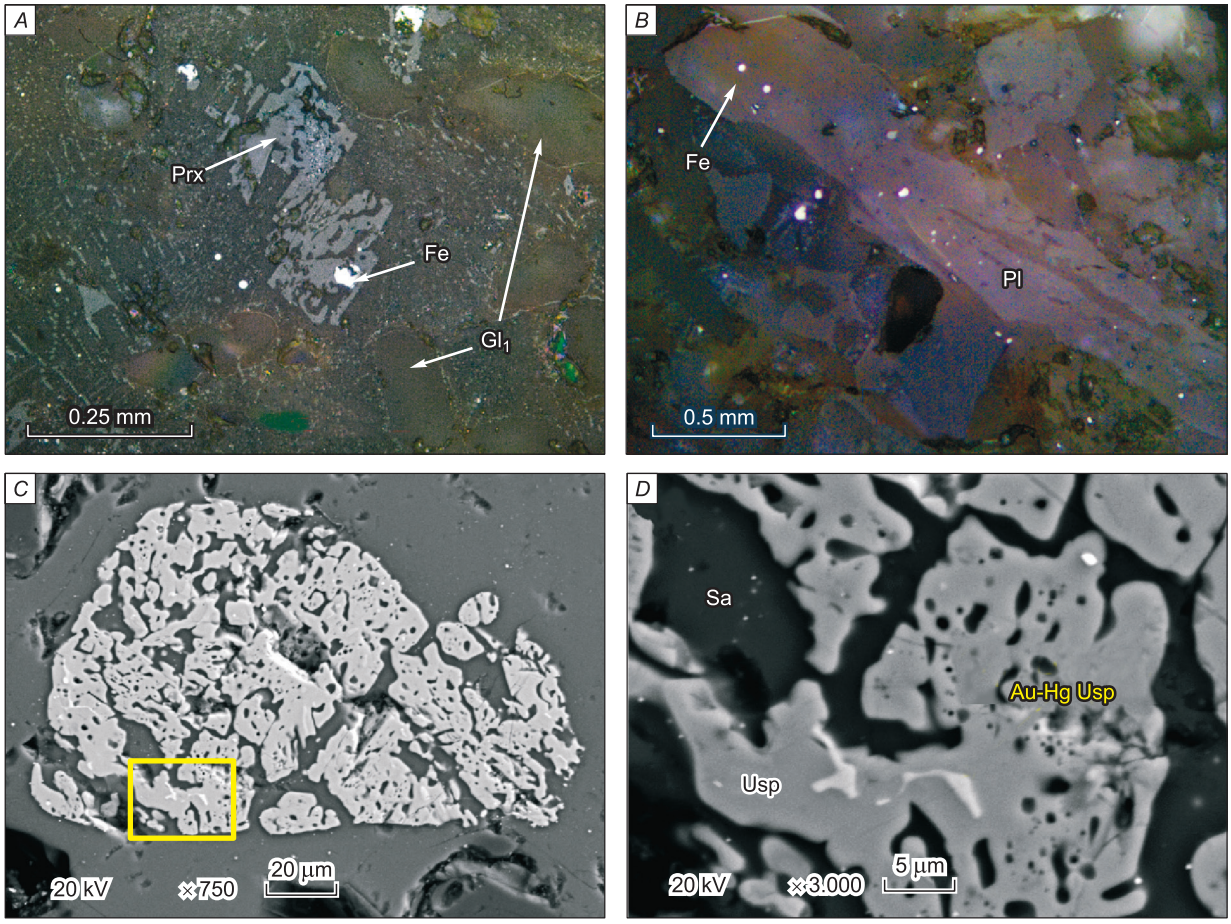

Fig. 11. A – Close-up photomicrograph of skeletal clinopyroxene phenocryst with melt inclusion of native iron. Matrix is a variolitic andesite (sample 1044). *B* – Close-up photomicrograph of plagioclase phenocryst with melt inclusion of native iron. Matrix is a variolitic andesite (sample 1044). *C* – Back-scattered electron image showing titaniferous magnetite skeletal crystal in glass matrix (microprobe analysis in table 2). Yellow rectangle shows the location of figure 11D. *D* – Detail back-scattered electron image of figure 11C, showing Au-Hg-rich phase in titaniferous magnetite. Abbreviations: Gl_1 – Globule-1; Fe – native iron; Prx – Pyroxene; Pl – Plagioclase; Sa – Sanidine; Usp – Ulvospinele.

Table 2

Microprobe analysis of the spinel-group minerals in titaniferous magnetite iron ore

MgO	Al_2O_3	TiO_2	FeO_{tot}	Au	Hg	Total
5.84	4.67	70.2	17.53	–	–	98.24
6.06	4.16	69.62	19.16	–	–	99.00
5.81	3.88	69.92	19.13	–	–	98.74
3.92	1.89	75.71	18.25	–	–	99.77
4.34	4.98	71.43	17.99	–	–	98.74
6.49	5.9	73.73	13.37	–	–	99.49
5.57	7.28	68.83	16.44	–	–	98.12
1.29	3.26	76.36	7.46	6.85	2.91	98.13
2.8	2.13	75.17	3.2	3.54	3.49	90.33

2. **Magnetite lava** contains of the magnetic fraction from 25 to 37 % of the total volume. In magnetite-rich lavas the FeO_{tot} content can reach 70.8 %, and ultra-rich magnetite lava (sample 1042/3, Table 1) shows 94.08 % of FeO_{tot}. According to the total composition (in %): SiO_2 – 36.32, TiO_2 – 0.62, Al_2O_3 – 11.83, Fe_2O_3 – 16.99, FeO – 4.47, MnO – 0.66, MgO – 1.95, CaO – 17.08, Na_2O – 0.54, K_2O – 1.16, H_2O^- – 1.21, H_2O^+ – 1.8, LOI – 2.14, P_2O_5 – 0.03, CO_2 – 1.62, S – 1.55 lava corresponds to melilititic and melilite-bearing volcanic rock. The lava mineral assemblage made up of melilite (prevail) + clinopyroxene + feldspathoids + hyalophane or celsian. All magnetite crystals trapped in the silicate matrix, composed (in %) of: SiO_2 – 35.5, TiO_2 – 0.9, Al_2O_3 – 7.5, FeO_{total} – 13.96, MgO – 3.91, CaO – 37.38, Na_2O – 0.45, K_2O – 0.75.

This type of magnetite comprises that of the main massive magnetite mineralization at Kildyam. Magnetite-A (Table 3) and is dominated by the (Mg–Al–Ti–Mn)-poor compositions. This depletion in MgO, Al_2O_3, TiO_2 and MnO is much more pronounced if compared to the magnetite-B (Figure 12, *D*).

Table 3

Microprobe analysis of the spinel-group minerals in magnetite lava

MgO	Al_2O_3	TiO_2	MnO	FeO_{tot}	Total
Magnetite-A – main mineral phase					
–	3.05	2.2	1.58	92.63	99.7
–	2.28	4.01	2.87	91.04	98.86
–	2.32	3.22	2.81	91.35	100.21
–	2.52	2.44	1.86	92.04	99.64
–	2.88	1.27	1.63	94.43	100.21
2.37	4.08	0.98	1.24	90.97	99.64
2.14	3.49	0.95	1.32	89.58	97.48
0.6	2.71	1.87	1.85	92.37	99.4
1.0	3.79	1.02	1.49	92.1	99.4
3.99	10.86	–	–	85.6	100.45
4.77	11.3	–	–	83.67	99.74
3.78	11.72	–	–	83.83	99.33
2.58	9.58	–	–	86.87	99.03
Magnetite-B – inclusions in the main mineral phase					
–	8.84	16.74	1.62	69.32	96.52
–	8.07	16.4	1.46	68.73	94.66
–	5.76	20.97	1.95	68.29	96.97
–	4.14	21.6	2.13	69.96	97.83
–	5.75	21.73	1.85	69.87	99.2
11.15	–	–	27.8	59.32	98.27
8.57	–	–	29.19	58.59	96.35
11.39	–	–	28.37	58.74	98.5
14.28	–	–	25.3	60.87	100.45
12.01	–	–	24.67	60.98	97.66
11.62	–	–	24.76	61.23	97.61
13.6	–	–	24.89	60.71	99.2
13.05	–	–	24.8	60.69	98.54
11.71	–	–	23.9	62.52	98.13
13.26	–	–	25.72	59.4	98.38

Discussion

Field evidence from Kildyam Volcanic Complex is interpreted to show important role of fracture tectonics for the penetration of magmatic melts. Due to the fracture nature of the outpouring lavas and fluid-magmatic differentiation of the melts, volcanic formation is separated to dacitic and andesitic. A microprobe area scan of the matrix of magnetite lavas allowed to determine its chemical composition (Table 4) in addition to the table 1.

The combined plot of chemical makeup and microprobe areal scanning of the lavas (Fig. 13, *A*) shows the basic trend defined by the composition of the Kildyam volcanic rocks. The low silicate iron-enriched pyroxenites and iron-depleted melilitites are particularly interesting. Olivine-clinopyroxenite includes about 6.07 % of magnetite that makes it similar to kosvite and looking alike the deposits of Iron Oxide Copper-Gold (IOCG) style close to the Kiruna-type. It can be assumed that the pyroxenite melt was divided into magnetite lavas and melilitites, as a result of fractionation. Further melt differentiation led to the isolation of native iron and trachyandesite glass from the andesitic melt.

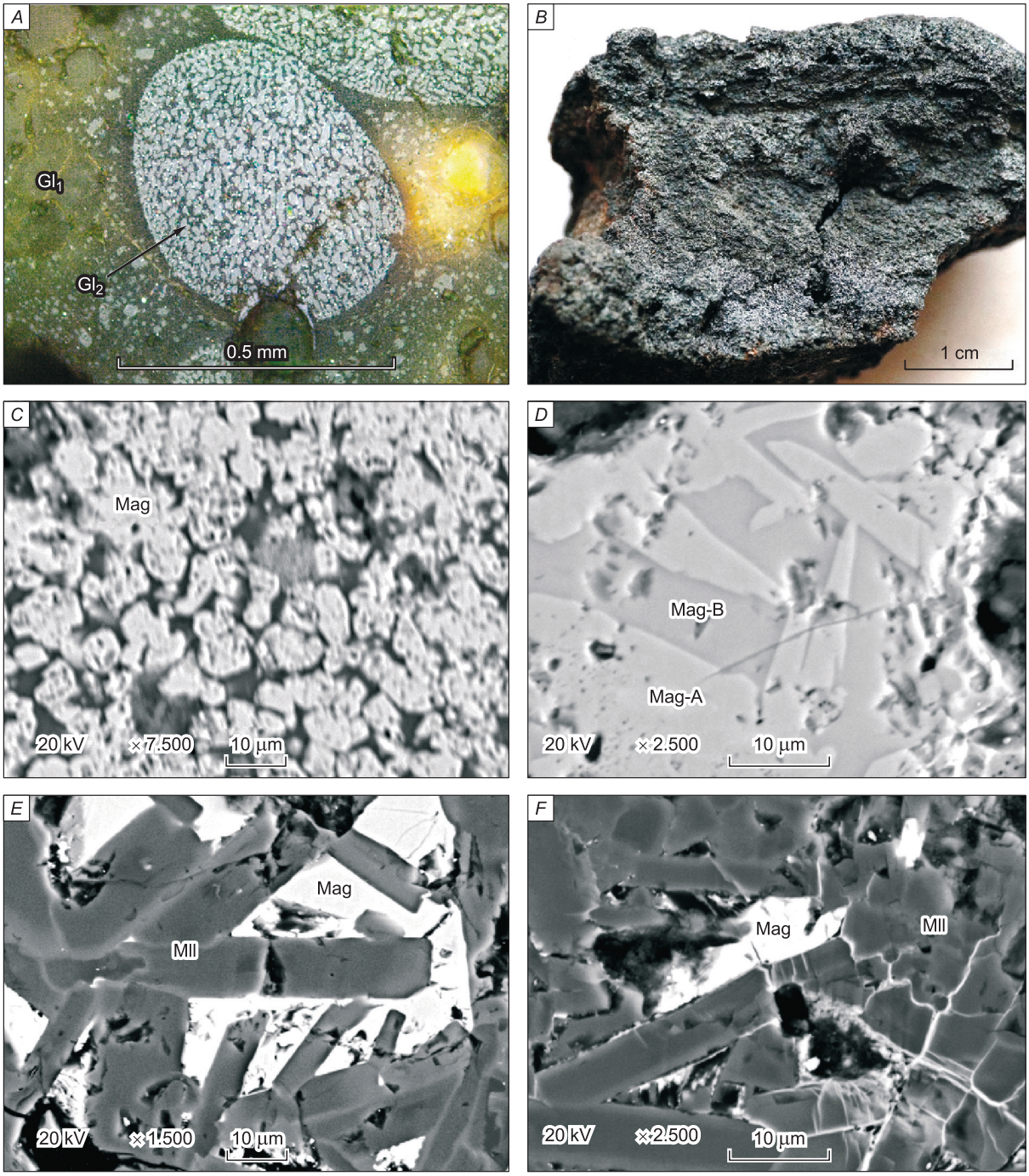

Fig. 12. Magnetite lava minerals assemblage.
A – Magnetite globule (Gl_2) with melilitite matrix in variolitic lava (sample 1044). *B* – High grade magnetite-lava (sample 1042/3, Table 1). *C* – Back-scattered electron image, showing magnetite-A – main mineral phase (microprobe analysis in table 3). *D* – Detail back-scattered electron image of fig. 12, *C*, showing Mn- and Al–Ti-rich phases in magnetite. *E* and *F* – Back-scattered electron images of melilite matrix filled with magnetite and depleted with magnetite. Abbreviations: Gl_1 – Globule-1; Mag – Magnetite; Mag-A – Magnetite-A; Mag-B – Magnetite-B; Mll – Melilite.

The behavior of iron defines the calc-alkaline and tholeiitic trends. Chin E.J. et al illustrated [30] that magmas evolving along the calc-alkaline trend move towards Fe-depletion, whereas magmas evolving along the tholeiitic trend become Fe-enriched. Our research confirmed that tholeiitic trend of iron-rich pyroxenites evolves towards two immiscible liquids – magnetite lava and melilitite matrix. Fur-

Table 4

Microprobe areal scanning analysis of variolitic lavas (in %)

SiO_2	TiO_2	Al_2O_3	FeO_{tot}	MgO	CaO	Na_2O	K_2O	Pt	Total
Glassy variolitic matrix									
61.48	0.61	12.05	8.65	1.26	11.38	3.25	1.96	–	100.64
56.54	0.78	14.37	5.11	2.28	17.56	2.24	1.33	–	100.21
56.21	0.73	14.41	3.8	2.45	17.01	2.37	1.6	–	98.58
58.69	0.84	15.66	3.76	1.08	16.31	2.61	1.95	–	100.9
58.68	0.89	13.68	4.01	2.35	16.5	2.49	1.66	–	100.26
Microcristalline matrix with iron and troilite globules									
54.73	1.49	19	12.79	–	2.31	5.17	4.52	0.67	100.68
55.37	1.28	18.06	13.21	–	2.31	4.74	4.7	0.62	100.29
56.17	1.32	18.21	11.97	–	2.02	4.94	4.71	0.95	100.29
Melilitic matrix in magnetite lavas									
35.5	0.9	7.5	13.96	3.91	37.38	0.45	0.75	–	100.35
36.37	–	6.43	10.95	2.22	43.88	0.5	0.21	–	100.56
35.24	0.98	7.98	12.77	3.3	36.9	0.94	0.73	–	98.84
34.73	–	10.14	9.08	5.05	37.96	0.61	0.2	–	97.77

Table 5

Microprobe analysis of ore minerals in variolitic andesites, %

Sample	Fe	Co	Ni	Au	Ag	Pt	Ir	S	Total
Iron native									
1030/4	97.23	2.24	–	–	–	0.11	–	–	99.58
1030/4	98.57	2.23	–	–	–	–	–	–	100.8
1030/4	96.08	1.98	1.09	–	–	–	–	–	99.15
1030/4	97.32	1.77	0.47	–	–	0.53	–	–	100.09
1030/4	94.96	1.24	–	1.31	–	–	0.28	–	97.79
1030/4	96.97	1.03	0.12	0.95	–	–	–	–	99.07
1030/4	95.05	0.89	–	2.52	–	–	2.1	–	100.56
Troilite									
1030/1	60.35	–	–	1.47	–	1.31	0.57	34.76	98.46
1030/4	59.72	–	–	1.4	–	0.53	–	36.36	98.01
1030/1	60.31	–	–	1.33	–	0.46	0.81	36.67	99.58
1030/4	61.17	–	–	1.12	–	–	–	36.31	98.6
Pyrite									
1030	48.37	–	–	2.71	0.28	1.22	1.64	44.33	98.55
1030	47.79	–	–	0.83	–	0.79	–	47.23	96.64
1030	49.52	–	–	0.69	–	1.61	–	47.49	99.31

ther evolution leads to the separation of native iron and the transition of lavas to the calc-alkaline trend (Fig. 13, B).

REE element data is reported in table 1. The ΣREE is low variable, ranging from 225.54 ppm to 329.43 ppm in red tuffs, from 235.29 ppm to 309.3 ppm in dacites, from 453.69 ppm to 462.77 ppm in andesites, 172.36 in pyroxenite and 102.12 in magnetite lava. Europium anomaly Eu/Eu* is ranging from 0.2 to 0.24 in red tuffs, from 0.2 to 0.25 in dacites, from 0.2 to 0.24 in andesites, 0.18 in pyroxenite and 0.26 in magnetite lava. Rare-earth geo-

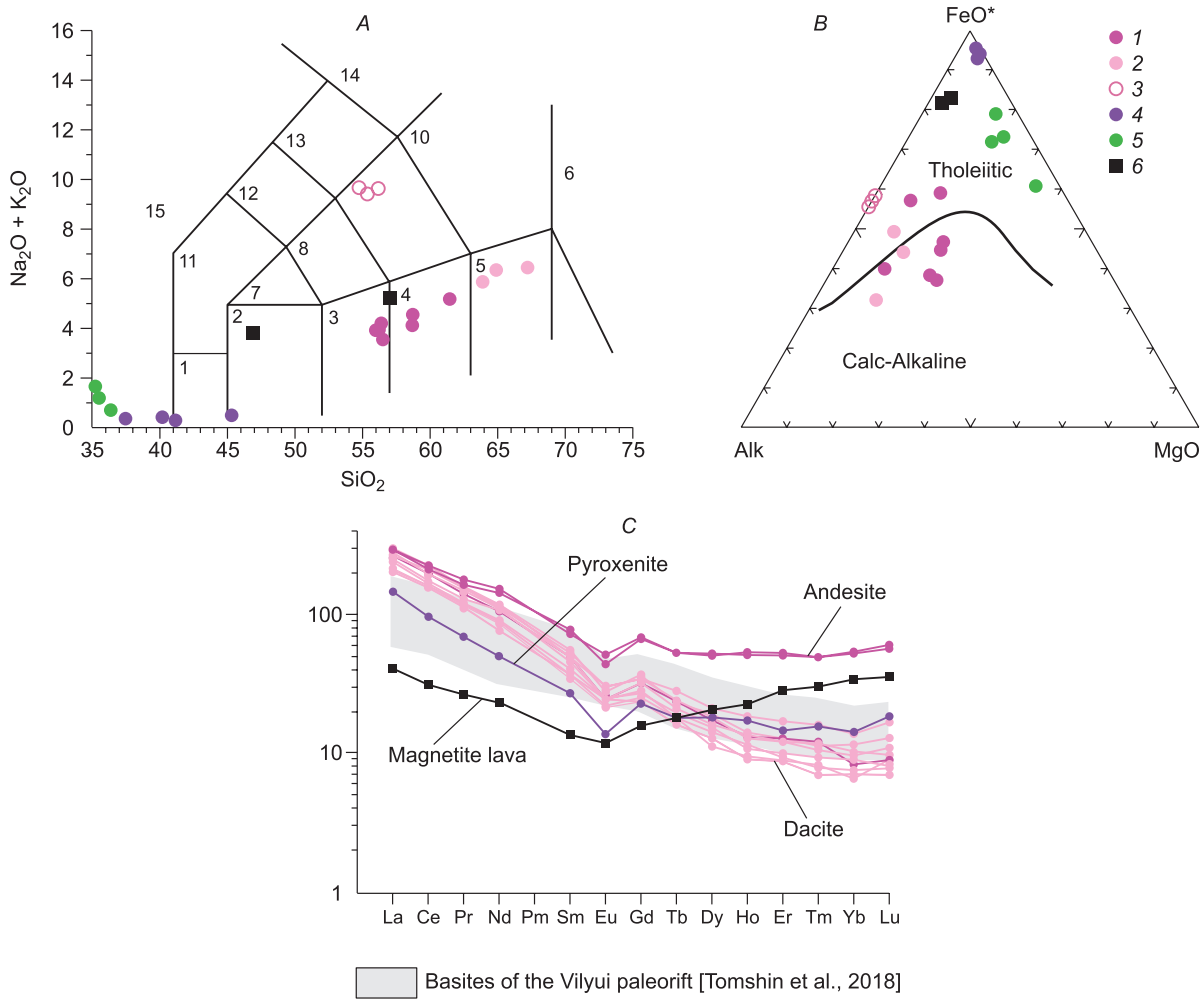

Fig. 13. Variation diagrams for the Kildyam volcanic rocks associated with iron-rich mineralization:
A – SiO_2 – K_2O+Na_2O TAS diagram after LeBas et al. [31] showing the trend defined by the composition of Kildyam volcanic rocks. Areas on the graph: 1 – Picrobasalt, 2 – Basalt, 3 – Basaltic andesite, 4 – Andesite, 5 – Dacite, 6 – Rhyolite, 7 – Trachybasalt, 8 – Basaltic trachyandesite, 9 – Trachyandesite, 10 – Trachyte-trachydacite, 11 – Tephrite Basanite, 12 – Phonotephrite, 13 – Tephriphonolite, 14 – Phonolite, 15 – Foidite. *B* – AFM-diagram after Irvine and Baragar [32] for the Kildyam volcanic rocks, showing the relative proportions of the oxides Na_2O + K_2O (Alk), FeO + Fe_2O_3 (FeO*) and MgO. *C* – Chondrite normalized REE diagram for the Kildyam volcanic rocks after Sun and McDonough [33]. Legend for volcanic rocks: *1* – dacite bulk, *2* – andesite bulk, *3* – andesitic matrix with native iron globules, *4* – pyroxenite, *5* – melilitite matrix in magnetite lava, *6* – magnetite lava.

chemical system of the Kildyam volcanic rocks is characterized by behavior close to the CHARAC (CHArge-and-RAdius-Controlled)-system (26<Zr/Hf<46 и 24<Y/Ho<34) where H/Ho – Zr/Hf ratios of the pair show the distribution close to chondrite (Zr/Hf – 36.6 and Y/Ho – 27.7) [34]. The distribution of Zr/Hf ratio in red tuffs differs from 18.59 to 23.87 and Y/Ho – from 25.38 to 28.48. The distribution of Zr/Hf ratio in dacites differs from 18.71 to 26.04 and Y/Ho – from 22.98 to 27.83. The distribution Zr/Hf ratio in andesites of differs from 31.22 to 31.62 and Y/Ho – from 34.14 to 35.61. The distribution of Zr/Hf ratio in pyroxenite is 30.24 and Y/Ho –28.25. The distribution of Zr/Hf ratio in andesites differs from 31.22 to 31.62 and Y/Ho – from 34.14 to 35.61. The distribution of Zr/Hf ratio in pyroxenite is 70.27 and Y/Ho – 26.91.

Chondrite normalized REE diagram for the Kildyam volcanic rocks (Fig. 13, C) with included data after M.D. Tomshin et al. [35] for the basites of Vilyui paleorift (see Fig. 1) showing similar REE geochemistry. This may indicate the unified nature of the source of Kildyama lavas and basitic magma.

Table 6

Microprobe analysis of ore minerals in pyroxenites, %

Fe	S	Au	Ag	Pt	Total
Troilite					
63.28	36.14	1.54	–	–	100.96
61.61	36.27	0.48	–	0.85	99.21
61.39	36.58	–	–	1.28	99.25
60.68	36.45	–	–	0.52	97.65
60.26	38.01	1.23	–	1.32	100.82
60.2	37.68	–	–	1.23	99.11
60.08	36.85	1.74	–	1.57	100.24
58.66	38.51	1.07	0.15	2.04	100.43
58.54	36.81	3.15	1.68	0.73	100.91
58.48	37.09	0.38	–	0.97	96.92
Pyrite					
48.12	48.03	0.21	–	2.16	98.52
47.52	48.47	–	0.31	0.88	97.18
46.65	51.56	–	–	1.56	99.77
46.1	49.57	0.97	–	0.57	97.21
45.85	52.38	2.25	–	–	100.48
45.69	47.88	–	–	2.88	96.45
44.9	50.61	0.51	–	1.87	97.89
44.73	50.05	–	1.18	1.1	97.06
44.55	52.45	0.86	–	1.52	99.38

In addition to magnetite variolitic andesites and pyroxenites are saturated Fe-minerals, the main ones are native iron, troilite and pyrite. According to microprobe analysis (Table 5 and Table 6) minerals contain impurities of Co, Ni, Pt, Ir, Au and Ag. Ag-bearing tetrahedrite (Table 7) inclusions detected in magnetite lava that fill the vesicles together with cristobalite.

Conclusions

Kildyam iron oxide deposit has been interpreted as lava flows and feeder dykes formed from iron-rich pyroxenite magma as a result of liquid immiscibility. Associated with andesitic lavas mineralization occur as massive, tabular bodies, stratified, pyroclastic ores. Our research confirmed that tholeiitic trend of iron-rich pyroxenites evolves towards two immiscible liquids – magnetite lava and melilitite matrix. Further evolution leads to the separation of native iron and the transition of lavas to the calc-alkaline trend. Petrographic and microprobe studies confirmed the liquid immiscibility in silicate melt during crystallization. Immiscible liquids are preserved as globules of one glass in another in andesites and as melt inclusions of native iron in matrix, clinopyroxene and plagioclase phenocryst.

Immiscibility of iron- and silica-rich melts during andesitic volcanism led to the formation of ex-

Table 7

Microprobe analysis of Ag-bearing tetrahedrite in vesicles from magnetite lava, %

Sample	Cu	Ag	Fe	Zn	Sb	As	S	Total
1064-1	31.69	7.16	5.23	5.55	25.28	2.16	23.89	100.96
1064-1	31.71	6.1	5.72	4.07	25.96	2.39	23.41	99.36
1064-1	31.71	6.19	5.08	5.82	24.72	1.74	24.45	99.71
1064-1	32.31	6.06	5.64	5.33	24.27	2.14	23.84	99.59
1064-1	31.59	7.06	5.87	5.92	24.78	1.26	23.93	100.41
1064-1	31.33	6.35	6.44	4.48	22.75	2.2	24.71	98.26
1064-1	32.48	6.6	5.37	5.77	24.43	1.95	24.04	100.64
1064-1	32.26	6.33	6.07	5.17	24.37	1.48	24.87	100.55
1064-1	33.76	6.53	5.73	4.04	24.56	2.28	24.02	100.92
1064-1	30.29	8.38	5.54	5.04	24.5	2.65	24.48	100.88
1064-1	31.58	5.73	5.03	4.07	25.34	1.44	24.11	97.3
1064-1	32.13	5.56	4.51	5.4	27.74	1.49	23.39	100.22
1064-1	32.79	5.71	5.28	5.97	26.17	1.46	22.01	99.39
1064-1	30.6	5.55	7.06	5.49	27.51	1.54	23.07	100.82
1064-1	32.1	5.47	4.73	5.94	29.27	1.81	21.32	100.64
1064-1	33.36	4.54	4.12	6.06	26.61	1.97	23.46	100.12
1064-1	32.37	5.72	5.41	3.56	25.78	1.43	24.77	99.04

otic varieties of magnetite-rich volcanic rocks. They have a lot of common features with the Kiruna type Pliocene El Laco volcano hosted iron oxide deposit. The good news for the project' economics is the proximity of the discovered iron-oxide ores in Mesozoic andesite-dacite lava flows to the city of Yakutsk.

This is only a beginning and there is lots of work to do. Further research should be associated with a detailed study of satellite imagery and characterization of the alteration of volcanic facies at regional to deposit scale, prospecting and mineralogy of associated Au, Ag, Cu, Fe, and REE ores.

References

1. *Kepezhinskas V.V., Luchitsky I.V.* Continental volcanic associations of Central Mongolia. 1974.

2. *Maslov V.K.* Gold in Jurassic deposits of the Vilyui syneclise // Geology and geophysics. 1995. Vol. 36(1).

3. *Kostin A.V., Grinenko V.S., Oleinikov O.B., Jelonkina M.S., Krivoshapkin I.I., Vasiljeva A.E.* The first data about the manifestation of the Upper Cretaceous volcanism of transition zone «Siberian platform – Verkhoyansk-Kolyma folded area» // Arctic and Subarctic Natural Resources. 2015. Vol. 1(77). P. 30–36. https://elibrary.ru/item.asp?id=23457540

4. *Kostin A.V., Trunilina V.A.* Volcanogenic creations of Kangalassky terrace (left bank of the Lena river. Central Yakutia) // Advances in Current Natural Sciences. 2018. Vol. 5. P. 92–100. https://doi.org/10.17513/use.36761

5. *Goldbraikh G.I., Todorovskaya V.N.* On the discovery of tufogenic rocks in the Lower Cretaceous sediments of the river basin. Sitte // Geology and oil and gas potential of Western Yakutia. Leningrad: Proceedings VNIGRI. 1966. Is. 249. P. 182–185.

6. *Kossovskaya A.G., Shutov V.D., Muravyov V.P.* Mesozoic and Upper Paleozoic sediments of the Western Verkhoyansk and Vilyui depression // Transactions of Geol. Institute of Academy of Sciences of the USSR. 1960. Vol. 34. 276 p.

7. *Kostin A.V.* A new geological feature of volcanic origin in the Lena-Vilyui watershed (East of Siberian platform) // Advances in Current Natural Sciences. 2017. Vol. 2. P. 100–105. https://doi.org/10.18411/a-2017-049

8. *Frietsch R.* On the magmatic origin of iron ores of the Kiruna type // Economic Geology. 1978. Vol. 73(4). P. 478–485. http://doi.org/10.2113/gsecongeo.73.4.478

9. *Hitzman M.W., Oreskes N., Einaudi M.T.* Geological characteristics and tectonic setting of proterozoic iron oxide (Cu–U–Au–REE) deposits // Precambrian Research. 1992. Vol. 58. P. 241–287. https://doi.org/10.1016/0301-9268(92)90121-4

10. *Hou T., Charlier B., Namur O., Schütte P., Schwarz-Schampera U., Zhang Z., Holtz F.* Experimental study of liquid immiscibility in the Kiruna-type Vergenoeg iron–fluorine deposit. South Africa // Geochimica et Cosmochimica Acta. 2017. Vol. 203. P. 303–322. https://doi.org/10.1016/j.gca.2017.01.025

11. *Philpotts A.R.* Liquid immiscibility in silicate melt inclusions in plagioclase phenocrysts // Bulletin de Minéralogie. 1981. Vol. 104. P. 317–324.

12. *Philpotts A.R.* Compositions of immiscible liquids in volcanic rocks // Contributions to Mineralogy and Petrology. 1982. Vol. 80. P. 201–218.

13. *Tornos F., Velasco F., Hanchar J.M.* Iron-rich melts, magmatic magnetite, and superheated hydrothermal systems: The El Laco deposit. Chile // Geology. 2016. Vol. 44. P. 427–430. https://doi.org/10.1130/G37705.1

14. *Parfenov L.M., Prokopiev A.V., Gaiduk V.V.* Cretaceous frontal thrusts of the Verkhoyansk fold belt, eastern Siberia // Tectonics. 1995. Vol. 14(2). P. 342-358.

15. *Parfenov L.M., Kuzmin M.I. (Eds.)* Tectonics, Geodynamics, and Metallogeny of the Sakha Republic (Yakutia) Territory. Moscow, MAIK Nauka/Interperiodika: Russia. 2001. 571 p. ISBN 5-7846-0046-X. https://elibrary.ru/item.asp?id=22399198

16. *Grinenko V.S., Kamaletdinov V.A., Shcherbakova O.I.* Section correlation scheme // Geological map of Yakutia on a scale of 1: 500.000. Central Yakutsk block. Sheet P-51-A. B. SPb.: St. Petersburg Card Factory, VSEGEI. 2000.

17. *Grinenko V.S.* Cretaceous continental formations of the east of the Siberian platform // Otechestvennaya Geologiya. 2007. Vol. 1. P. 110–118.

18. *Grinenko V.S., Knyazev V.G.* New data on stratigraphy and zoning of Jurassic deposits of the western periphery of the Verkhoyansk-Kolyma folded region // Bulletin of the State Committee for Geology. Materials on geology and minerals of the Republic of Sakha (Yakutia). 2010. Vol. 1 (9). P. 26–38.

19. *Smelov A.P., Andreev A.P., Altukhova Z.A., Babushkina S.A., Bekrenev K.A., Zaitsev A.I., Izbekov E.D., Koroleva O.V., Mishnin V.M., Okrugin A.V., Oleinikov O.B., Surnin A.A.* Kimberlites of the Manchary pipe: a new kimberlite field in Central Yakutia // Russian Geology and Geophysics. 2010. Vol. 51(1). P. 153–159.

20. *Polyansky O.P., Prokopiev A.V., Koroleva O.V., Tomshin M.D., Reverdatto V.V., Babichev A.V., Sverdlova V.G., Vasiliev D.A.* The nature of the heat source of mafic magmatism during the formation of the Vilyui rift based on the ages of dike swarms and results of numerical modeling // Russian Geology and Geophysics. 2018. Vol. 59. P. 1217–1236. http://dx.doi.org/10.1016/j.rgg.2018.09.003

21. *Afanasiev V.P., Pokhilenko N.P., Grinenko V.S., Kostin A.V., Malkovets V.G., Oleinikov O.B.* Kimberlitic magmatism in the south-western flank of the Vilui basin // RAS reports. Earth sciences. 2020. Vol. 490(2). P. 5–9. http://dx.doi.org/10.7868/S2686739720020036

22. *Smelov A.P., Surnin A.A.* Gold of the city of Yakutsk // Science First Hand. 2010. Vol. 4(34). P. 16–19.

23. *Grinenko V.S., Kostin A.V., Kirichkova A.I., Zhelonkina M.S.* Boundary Upper Jurassic-Lower Cretaceous rocks in the eastern Siberian craton: New data // Vestnik Voronezhskogo Gosudarstvennogo Universiteta. Ser.: Geologiya. 2018. Vol. 2. P. 48–55. https://doi.org/10.18411/vgu-sg-2018-2-48-55

24. *Silber A., Bar-Yosef B., Singer A., Chen Y.* Mineralogical and chemical composition of three tuffs from northern Israel // Geoderma. 1994. Vol. 63(2). P. 123–144. https://doi.org/10.1016/0016-7061(94)90002-7

25. *Stück H., Forgó L.Z., Rüdrich J., Siegesmund S., Török A.* The behaviour of consolidated volcanic tuffs: weathering mechanisms under simulated laboratory conditions // Environmental geology. 2008. Vol. 56(3-4). P. 699–713. https://doi.org/10.1007/s00254-008-1337-6

26. *Horwell C.J., Williamson B.J., Llewellin E.W., Damby D.E., Le Blond J.S.* The nature and formation of cristobalite at the Soufrière Hills volcano. Montserrat: implications for the petrology and stability of silicic lava domes // Bulletin of Volcanology. 2013. Vol. 75(3). 696 p. https://doi.org/10.1007/s00445-013-0696-3

27. *Reich M., Zúñiga A., Amigo Á., Vargas G., Morata D., Palacios C., Parada A.M., Garreaud R.D.* Formation of cristobalite nanofibers during explosive volcanic eruptions // Geology. 2009. Vol. 37(5). P. 435–438. https://doi.org/10.1130/G25457A.1

28. *Schipper C.I., Castro J.M., Tuffen H., Wadsworth F.B., Chappell D., Pantoja A.E., Simpson M.P., Le Ru E.C.* Cristobalite in the 2011–2012 Cordón Caulle eruption (Chile) // Bulletin of Volcanology. 2015. Vol. 77(5). P. 5–34. https://doi.org/10.1007/s00445-015-0925-z

29. *Kostin A.V., Trunilina V.A., Grinenko V.S.* Geological model of the Tyugeninsky field of volcanic rocks (east of the Siberian platform) // Geology and mineral resources of the North-East of Russia: materials of the VII All-Russian scientific and practical conference dedicated to the 60th anniversary of the Institute of Geology of Diamond and Noble Metals of the Siberian Branch of the Russian Academy of Sciences. April 5–7 2017: in 2 volumes. Yakutsk: SVFU Publishing House, 2017. V. 2. P. 154–160. https://www.elibrary.ru/item.asp?id=30628694

30. *Chin E.J., Shimizu K., Bybee G.M., Erdman M.E.* On the development of the calc-alkaline and tholeiitic magma series: A deep crustal cumulate perspective // Earth and Planetary Science Letters. 2018. V. 482. P. 277–287. https://doi.org/10.1016/j.epsl.2017.11.016

31. *LeBas M.J., LeMaitre R.W., Streckeisen A. and Zanetin B.* A chemical classification of vofcanic rocks based on the total alkali-silica diagram // J. Petrol. 1986. Vol. 27. P. 745–750.

32. *Irvine T.N., Baragar W.R.* A guide to the chemical classification of the common volcanic rocks // Canadian Journal of Earth Sciences. 1971. Vol. 8. P. 523–548. https://doi.org/10.1139/e71-055

33. *Sun S.S., McDonough W.F.* Chemical and isotopic systematics of oceanic basalts: implications for mantle composition and processes // Geological Society. London. Special Publications. 1989. Vol. 42(1). P. 313–345.

34. *Bau M.* Controls on the fractionation of isovalent trace elements in magmatic and aqueous systems: evidence from Y/Ho. Zr/Hf. and lanthanide tetrad effect // Contributions to Mineralogy and Petrology 1996. Vol. 123(3). P. 323–333. https://doi.org/10.1007/s004100050159

35. *Tomshin M.D., Kopylova A.G., Konstantinov K.M., Gogoleva S.S.* Basites of the Vilyui paleorift: geochemistry and sequence of intrusive formation // Russian Geology and Geophysics. 2018. Vol. 59(10). P. 1204–1216. https://doi.org /10.1016/j.rgg.2018.09.002

Received 26.02.2020
Accepted 18.05.2020

About the author

KOSTIN Aleksey Valentinovich, doctor of geological and mineralogical sciences, head of laboratory, Diamond and Precious Metal Geology Institute, SB RAS, 39 Lenina pr., Yakutsk, 677980, Russia, https://orcid.org/0000-0002-5778-6505, a.v.kostin2006@rambler.ru

Citation

Kostin A.V. Immiscible silica- and iron-rich melts at the Kildyam volcano complex (central Yakutia, Russia)// Arctic and Subarctic Natural Resources. 2020. Vol. 25, No. 2. P. 25–44. https://doi.org/10.31242/2618-9712-2020-25-2-2